

Absorption and magneto-optical properties of the  ${}^3A_{2g} \rightarrow {}^1T_{2g}^a$  transition in  $\text{CsNiF}_3$ 

E. Imppu, R. Laiho, and T. Levola

*Wihuri Physical Laboratory, University of Turku, SF-20500 Turku 50, Finland*

T. Tsuboi

*Wihuri Physical Laboratory, University of Turku, SF-20500 Turku 50, Finland  
and Physics Department, Kyoto Sangyo University, Kamigamo, Kyoto 603, Japan\**

(Received 13 December 1983; revised manuscript received 13 March 1984)

Optical absorption, magnetic circular dichroism, and Faraday rotation have been investigated in the region of the spin-forbidden transition  ${}^3A_{2g} \rightarrow {}^1T_{2g}^a$  in the one-dimensional ferromagnet  $\text{CsNiF}_3$ . At low temperatures where magnetic short-range interactions are important, this band shows an anomalous increase of intensity with decreasing temperature. Below 40 K, a number of small peaks are observed on the low-energy side of the broadband absorption. From their temperature and magnetic field dependences the most prominent features were identified to be exciton lines associated with the  ${}^3A_{2g} \rightarrow {}^1T_{2g}^a$  transition. On the low-energy side of these lines, a "hot"-magnon band was identified on the basis of its position and the intensity which shows a linear increase with increasing temperature until a saturation is observed at about 12 K. From a comparison between the temperature dependence of the Faraday rotation and the existing susceptibility data of  $\text{CsNiF}_3$ , it was concluded that the Faraday rotation is directly proportional to the magnetization of the crystal.

## I. INTRODUCTION

The crystal structure of  $\text{CsNiF}_3$  is hexagonal (space group  $P6_3/mmc$ ).<sup>1</sup> It consists of  $\text{NiF}_6$  octahedra arranged along the  $c$  axis and Cs ions located in the space between the chains formed by these octahedra. Along the chains there is a ferromagnetic interaction between the  $\text{Ni}^{2+}$  ions, which determines the magnetic behavior of the crystal. In addition, there is a weak interchain interaction which leads to a three-dimensional (3D) antiferromagnetic ordering at  $T_N = 2.61$  K.<sup>2</sup> Above  $T_N$ ,  $\text{CsNiF}_3$  is a good example of a one-dimensional (1D) easy-magnetization-plane ferromagnet. In this phase the magnetic properties of the crystal are controlled by the correlation length  $\xi(T)$  of the spins, which determines the region over which the system can be considered to be magnetically ordered.

Owing to the combined effects of the trigonal distortion of the  $\text{NiF}_6$  octahedra along the  $c$  axis, the spin-orbit mixing from the upper states, and the exchange interaction, the ground state of the  $\text{Ni}^{2+}$  ions must be regarded as a mixture of the  $\Gamma_1^+$  and  $\Gamma_3^+$  components of the  ${}^3A_{2g}$  state.<sup>3</sup> In the near ir and the red regions of the spectrum the optical absorption of  $\text{CsNiF}_3$  is governed by the crystal-field transitions  ${}^3A_{2g} \rightarrow {}^3T_{2g}^a$ ,  ${}^3T_{1g}^a$ , and  ${}^1E_g$ . The zero-phonon pure-exciton line corresponding to the transition  ${}^3A_{2g} \rightarrow {}^3T_{2g}^a$  has been investigated in detail by Cibert *et al.*<sup>4,5,6</sup> It was shown that the zeroth, first, and second moments of this band can be related to various spin correlation functions. In particular, the unusual linear temperature dependence of the absorption peak position was attributed to the 1D ferromagnetic character of the crystal. Abdalian *et al.*<sup>7</sup> have used the electronic Raman scattering method to observe the transitions  ${}^3A_{2g} \rightarrow {}^3T_{2g}^a$  and  ${}^3T_{1g}^a$ . Both exciton and single-ion descriptions were applied in this work to identify sharp components of the

bands.

In magnetic crystals, spin-forbidden transitions may reveal features which are attributable to their spin dynamics. Such transitions may become allowed by spin-orbit mixing or by virtue of exciton-magnon interactions. In two sublattice antiferromagnets both "cold"- and "hot"-magnon bands are allowed.<sup>8,9</sup> In a ferromagnet where a decrease of the total spin projection is associated with an excitonic transition, a thermally created magnon must be simultaneously annihilated to conserve the total spin of the crystal. Consequently, only a hot-magnon band can be observed in ferromagnetic compounds. Most investigations of exciton-magnon combination bands in ferromagnets have been made in crystals which have two-dimensional (2D) magnetic interactions. Schnatterly and Fontana<sup>10</sup> have observed a hot-magnon band in  $\text{FeCl}_2$ , which is an antiferromagnet containing, however, alternating planes with parallel spins. In addition to this work the intensity of the hot-magnon band was investigated in a group of 2D ionic ferromagnets of the type  $A_2\text{CrX}_4$  ( $A$  denotes an alkali cation or  $\text{RNH}_3^+$ ;  $X$  denotes Cl or Br)<sup>11,12</sup> and shown to obey approximately a  $T^2$  law at low temperatures.

According to the numerical calculation of Ebara and Tanabe,<sup>13</sup> a hot-magnon band in a 1D ferromagnet should obey a roughly linear temperature dependence at low temperatures and saturate at a constant level at high temperatures. The first, and thus far probably the only, observation of a hot-exciton-magnon combination band in a 1D ferromagnet was made by Petit<sup>14</sup> around the transition  ${}^3A_{2g} \rightarrow {}^1T_{2g}^b$  in  $\text{CsNiF}_3$ . The energy of this band, however, shows that it probably has some phonon contribution, which makes it difficult to compare the temperature dependence of this band with the theoretical prediction.<sup>13</sup>

In  $\text{CsNiF}_3$  the spin-forbidden transition  ${}^3A_{2g} \rightarrow {}^1T_{2g}^a$  occurs around 460 nm. Although this transition lies on

the tail of a much stronger band due to spin-allowed transitions to the  ${}^3T_{1g}^b$  state, as usual in compounds containing  $\text{Ni}^{2+}$ , the transition seems to be useful in the investigation of magnetic interactions in a 1D ferromagnet. In this paper we shall first report the structure, the temperature dependence, and the magnetic-circular-dichroism (MCD) spectrum of the broadband absorption due to the transition  ${}^3A_{2g} \rightarrow {}^1T_{2g}^a$ . On the low-energy side of this band, a series of sharp, small peaks are observed. From their temperature and magnetic field dependences, both exciton and hot-magnon bands could be identified in the spectrum. Additionally, results of the Faraday-rotation (FR) measurements are reported and compared with the susceptibility data obtained by conventional methods.

## II. EXPERIMENTAL PROCEDURE

In these investigations, single crystals obtained from two different sources were used. For absorption measurements, (1–4)-mm-thick specimens, permitting investigations with the light propagating perpendicular to the (*a*, *c*) plane or along the *c* axis, were prepared. In order to reduce the effect of the demagnetizing field, a specimen with dimensions  $1 \times 2 \times 10 \text{ mm}^3$  was prepared for the FR measurements. Here, both the light beam and the external magnetic field were directed along the *c* axis of the crystal (parallel to the longest edge of the sample). Owing to the optical anisotropy of  $\text{CsNiF}_3$ , both the MCD and the FR measurements were made with a light beam propagating within  $1^\circ$  along the *c* axis. The right orientation was achieved by inspecting the sample crystal in a cryostat between a set consisting of a polarizer and an analyzer, and tilting and rotating the cryostat until a conoscopic cross was seen on a white card set behind the analyzer.

The temperature of the samples could be varied from 2 to 300 K by using either a He-immersion Dewar or a magneto-optical cryostat with the sample immersed in

He-exchange gas. The spectra were recorded in a single-beam spectrometer based on the use of a 150-W tungsten lamp and a Jarrel-Ash model no. 82-000 0.5-m Ebert monochromator. A combination of a Polacoat polarizer and a photoelastic modulator was used to obtain circularly polarized light for the MCD measurements.

## III. EXPERIMENTAL RESULTS

### A. Absorption measurements

Figure 1 shows the absorption spectra of  $\text{CsNiF}_3$  measured in the (*a*, *c*) plane using unpolarized light. The strong absorption in the near-uv region is attributable to the spin-allowed transition  ${}^3A_{2g} \rightarrow {}^3T_{1g}^b$ . On the low-energy side of this band, there is a much weaker band in the (440–480)-nm region which is identified to the spin-forbidden transition  ${}^3A_{2g} \rightarrow {}^1T_{2g}^a$ . This identification of the bands is confirmed by the fact that a quite similar absorption spectrum (including the band positions) is found for the  ${}^3T_{2g}^b$  and  ${}^1T_{2g}^a$  bands in other  $\text{Ni}^{2+}\text{-F}^-$  compounds such as  $\text{KNiF}_3$ ,<sup>15</sup>  $\text{Rb}_2\text{NiF}_4$ ,<sup>16,17</sup>  $\text{K}_2\text{NiF}_4$ ,<sup>17</sup> and  $\text{BaNiF}_4$ .<sup>18</sup> The temperature dependence of the absorption intensity (i.e., absorption area) of the  ${}^1T_{2g}^a$  band is shown in Fig. 2. The intensity of the  ${}^1T_{2g}^a$  band of  $\text{CsNiF}_3$  shows a tendency to decrease with increasing temperature as is observed for the spin-forbidden bands in  $\text{NiBr}_2$ ,<sup>19</sup>  $\text{NiCl}_2$ ,<sup>19</sup>  $\text{NiF}_2$ ,<sup>20</sup>  $\text{NaNiF}_3$ ,<sup>21</sup> and  $\text{KNiF}_3$ .<sup>22</sup> At temperatures above 70 K it is difficult to estimate the absorption intensity accurately because of strong overlapping by the phonon-assisted spin-allowed  ${}^3T_{1g}^b$  band which grows with increasing temperature at high temperatures.<sup>16,23</sup>

An additional small band is observed in the (520–540)-nm region in Fig. 1. The position of this band corresponds roughly to the combined energies of the transitions to the  ${}^3T_{2g}^a$  state [located around 1280 nm (Ref. 7)] and the  ${}^3T_{1g}^a$  state [around 840 nm (Ref. 7)]. Moreover, as de-

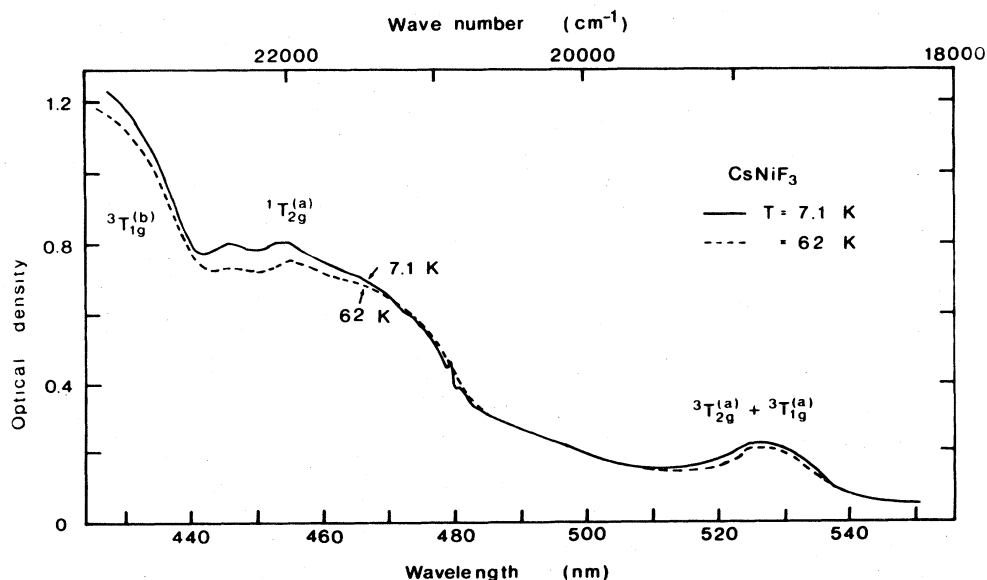


FIG. 1. Unpolarized absorption spectra of a 1-mm-thick  $\text{CsNiF}_3$  crystal in the visible and near-uv region.

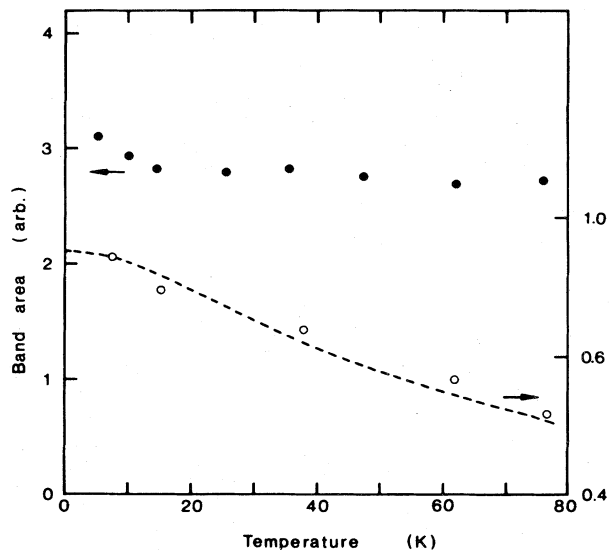


FIG. 2. Temperature dependence of the total area of the  ${}^3A_{2g} \rightarrow {}^1T_{2g}^{(a)}$  band (solid circles) and of the  $({}^3A_{2g} + {}^3A_{2g}) \rightarrow ({}^3T_{2g}^a + {}^3T_{1g}^a)$  double-exciton band (open circles). The dashed line gives the temperature dependence of the intensity corresponding to the double-excitonic transition  $({}^3A_{2g} + {}^3A_{2g}) \rightarrow ({}^1T_{2g}^a + {}^1T_{2g}^a)$  as observed by Petit (Ref. 14).

picted in Fig. 2, its temperature dependence obeys the behavior observed by Petit *et al.*<sup>24</sup> for the double-excitonic transitions  $({}^3A_{2g} + {}^3A_{2g}) \rightarrow ({}^1T_{2g} + {}^1T_{2g})$ , and  $({}^1E_g + {}^1E_g)$ . Therefore it is likely that the observed band is due to the double-excitonic transition  $({}^3A_{2g} + {}^3A_{2g}) \rightarrow ({}^3T_{2g}^a + {}^3T_{1g}^a)$ .

At low temperatures a number of small peaks, which we denote *A*, *B*, *C*, *D*, *E*, *F*, *G'*, and *G* in the order of increasing energy, are observed on the low-energy side of the  ${}^1T_{2g}^{(a)}$  broadband (Fig. 3). All these bands are seen in the  $\alpha$  spectrum ( $\vec{k} \parallel \hat{c}$ ,  $\vec{k}$  being the direction of propagation of light). The most distinct feature is that the *G* band peaking at  $(20879 \pm 5) \text{ cm}^{-1}$  is the strongest in the polarization  $\vec{E} \parallel \hat{c}$ , but can be seen also in the polarization  $\vec{E} \perp \hat{c}$ , while the *B*, *C*, and *F* bands are found only in the polarization  $\vec{E} \perp \hat{c}$  ( $\vec{k} \parallel \hat{a}$ ). Figure 4 shows the temperature dependence of the *A*-, *B*-, *C*-, and *G*-band intensities. The *A*-band intensity is almost constant at high temperatures but it decreases rapidly below about 12 K, approximately in proportion to the temperature. On the other hand, the *B*, *C*, *F*, and *G* bands can be observed only at temperatures below 35 K, where their intensities are found to increase linearly with temperature when the temperature is lowered. From such a rapid growth of the *B*, *C*, *F*, and *G* bands at low temperature, it can be concluded that the growth of the intensity of the total  ${}^1T_{2g}^{(a)}$  band observed below about 15 K (Fig. 2) is mainly due to the growth of these bands.

The *F* band at  $20809 \text{ cm}^{-1}$  is partially masked by the poorly resolved absorption bands *D* and *E* and is therefore difficult to investigate in detail. Instead, the low-energy bands *A* at  $20649 \text{ cm}^{-1}$ , *B* at  $20689 \text{ cm}^{-1}$ , and *C* at

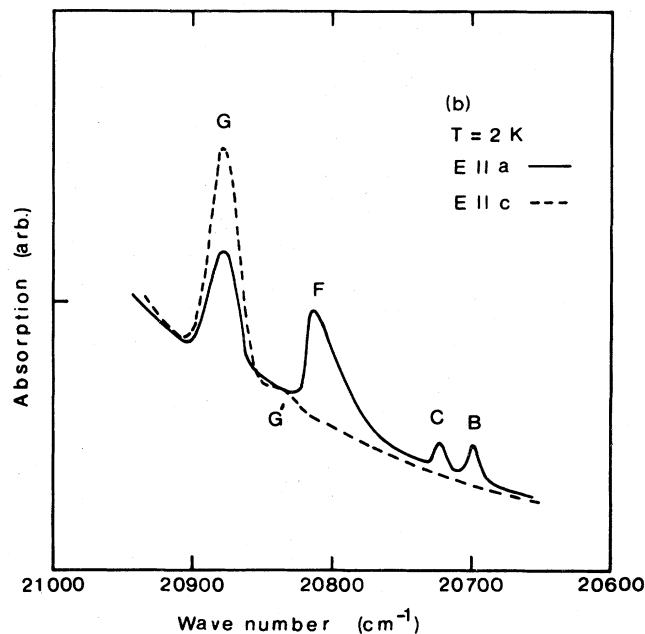
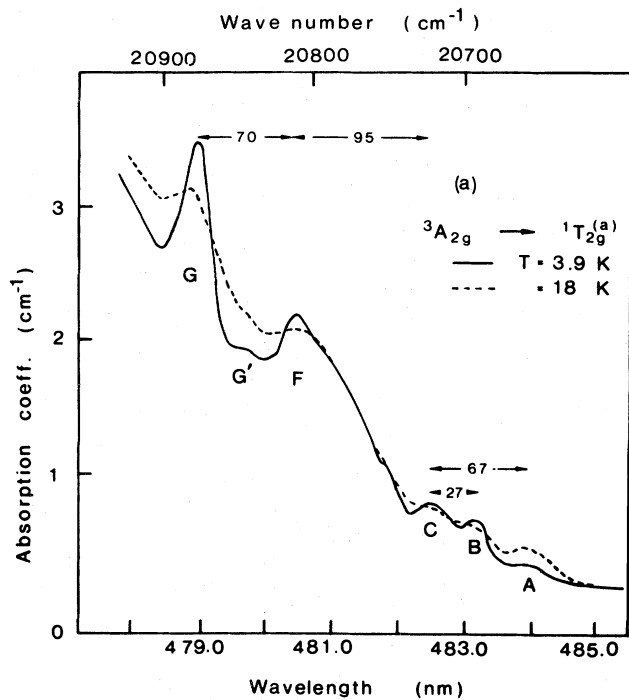


FIG. 3. (a) Fine structure observed on the low-energy tail of the  ${}^3A_{2g} \rightarrow {}^1T_{2g}^{(a)}$  band, measured with the geometry  $\vec{k} \parallel \hat{c}$ . The separations between the bands are given in units of  $\text{cm}^{-1}$ . (b) Polarization of the bands measured in the geometry  $\vec{k} \parallel \hat{a}$  and  $\vec{E} \parallel \hat{a}$  or  $\vec{E} \parallel \hat{c}$  and at the temperature  $T = 2 \text{ K}$ .

$20716 \text{ cm}^{-1}$  are better resolved although they still lie on the low-energy tail of the broad absorption band. Of the bands *A*–*G*, the sharp *G* band is the largest and it is easy to measure the peak position, the first moment, and the half-width of the *G* band. To experimental accuracy all

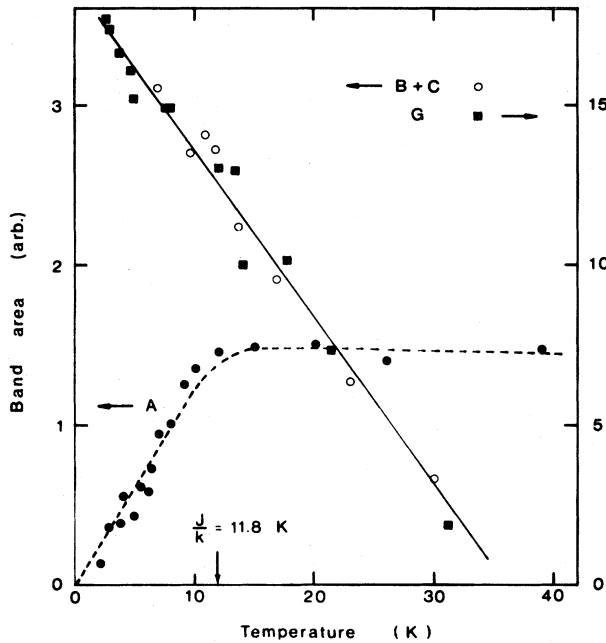


FIG. 4. Temperature dependences of the areas of the *A* band (solid circles), the *B* and *C* bands (open circles), and the *G* band (solid squares).

of these quantities have a linear temperature dependence. The slopes of the solid lines in Fig. 5 are  $-0.37k_B$  for the peak position,  $-0.71k_B$  for the first moment, and  $0.48k_B$  for the half-width where  $k_B$  is the Boltzmann constant. Figure 6 shows the variation of the *G* band when an external magnetic field is applied parallel to the *a* axis at 7 K. It is found that in the 1D ferromagnetic region the area of the *G* band is independent of the applied field. Instead, the peak position exhibits a blue shift with increasing field above 1 T and the half-width of the band is

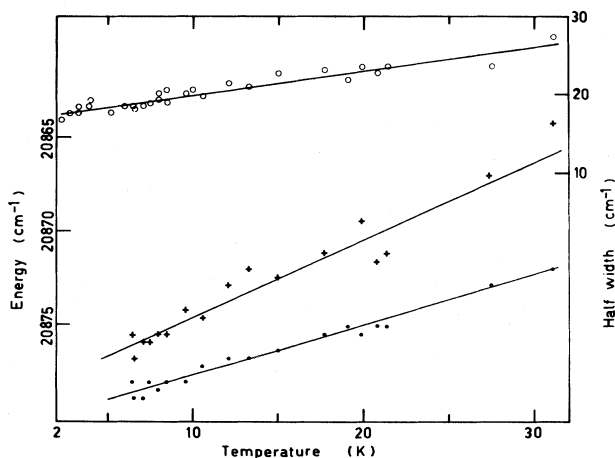


FIG. 5. Temperature dependence of the peak position (solid circles), the first moment (pluses), and the half-width (open circles) of the *G* band. Note that the half-width is given on the right-hand scale and indicates the full width at half-height of the band.

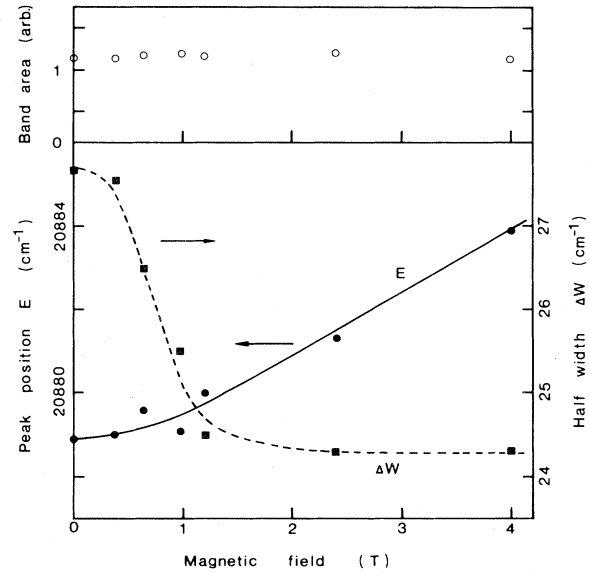


FIG. 6. Magnetic field dependence of the intensity (open circles), peak position (solid circles), and the half-width (solid squares) of the *G* band, measured at 7 K with  $\vec{H} \parallel \hat{a}$ .

reduced by about 10% in a field of 1 T. In measurements at 2 K, i.e., in the 3D antiferromagnetic region, no effect of the magnetic field on the half-width and position of the *G* band could be observed. As shown in Fig. 7, there is evidence that, unlike the *G* band, the weak *G'* band is reduced with increasing magnetic field. On the other hand, the *G'* band is found to grow with temperature at low temperatures like the *A* band, when no magnetic field is applied.

Figure 8 shows the temperature dependence of the *A*–*C* band region at low temperatures. An additional weak band, hereafter referred to as *A'*, is found on the

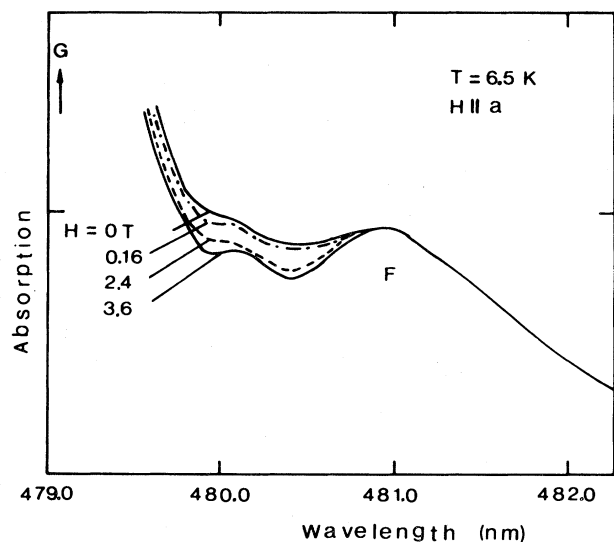


FIG. 7. Influence of the magnetic field applied along the *a* axis on the absorption at the low-energy side of the *G* band.

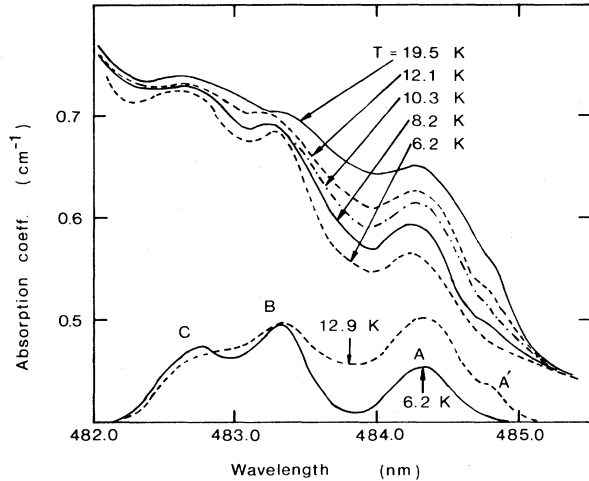


FIG. 8. Temperature dependence of the absorption spectra in the region of the  $A$ ,  $B$ , and  $C$  bands. In the lower part of the figure the absorption bands are shown after subtraction of the background.

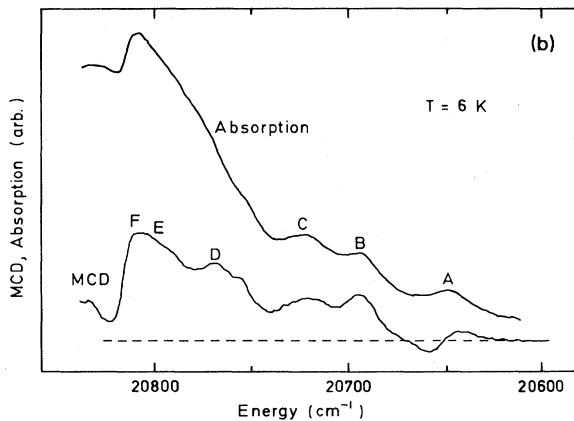
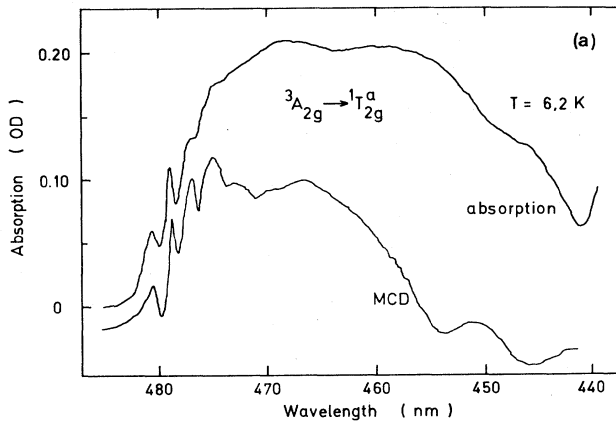


FIG. 9. (a) Magnetic-circular-dichroism spectrum of the broadband absorption  ${}^3A_{2g} \rightarrow {}^1T_{2g}^i$  where the two lowest-energy peaks are due to the  $F$  and  $G$  bands in the order of the increasing energy. MCD line of the small features observed on the absorption tail of the main band is shown in (b).

low-energy side of the  $A$  band. This band grows with increasing temperature as does the  $A$  band. The separation between  $A$  and  $A'$  is about  $18 \text{ cm}^{-1}$ . Although the  $A'$  band is clearly not found at low temperatures, such as  $6 \text{ K}$ , it is suggested from their common behavior that the  $A$  and  $A'$  bands arise from the same origin.

### B. MCD measurements

Magnetic-circular-dichroism absorption refers to differential absorption for left- and right-circularly-polarized light propagating along the direction of magnetization in matter. As can be seen from Fig. 9(a) the MCD line of the  ${}^3A_{2g} \rightarrow {}^1T_{2g}^i$  band and its most prominent low-energy components have the same shape as the corresponding absorption lines. The line shape of the MCD band is somewhat better resolved, clearly showing several peaks on the high-energy side of the  $G$  band. Presumably, this structure must be attributed to phonons since the separation of the first peak from the  $G$  band and the positions of the higher progression correspond to the energy of the phonons,  $74 \text{ cm}^{-1}$ , observed by Raman scattering.<sup>7</sup> Similarly, the MCD line shapes of the  $B$  and  $C$  bands coincide with the absorption-band shapes, but the  $A$  band has a derivativelike line shape [Fig. 9(b)]. This gives evidence, in addition to the different temperature dependence, that the transition mechanism behind the  $A$  band differs from that of the other features in this spectral region.

### C. Faraday rotation

In a paramagnetic nonabsorbing solid, the Faraday rotation is related to the off-diagonal elements in the dielectric tensor,  $\epsilon_{xy}(\omega) = 4\pi A i \chi H$ , where  $A$  is a constant,  $\chi$  is the susceptibility, and  $H$  is the magnetic field applied parallel to the path of light. For a unit length of the sample, the rotation of the polarization plane of the light is given by the angle

$$\theta = 4\pi^2 \lambda^{-1} n^{-1} \chi A H, \quad (1)$$

where  $\lambda$  is the wavelength of light and  $n$  is the refractive index in zero field.

In Fig. 10(a) the dispersion of the Faraday rotation is shown between  $450$  and  $600 \text{ nm}$ . While features originating from the transitions to the  ${}^1T_{2g}^i$  excited state are seen in the FR spectrum the dispersion is clearly influenced by transitions to the  ${}^3T_{1g}^i$  state. The MCD and FR measurements are complementary in the sense that the data obtained are connected via the Kramers-Kronig relation. However, the MCD spectra contain information on the positions, shapes, and intensities of individual absorption bands, whereas transitions to all of the excited states contribute to the FR spectra and less fine structure will usually be observed.

In the range of the magnetic field values used (from  $5 \times 10^{-3}$  to  $4.5 \text{ T}$ ),  $\theta$  was found to increase linearly with increasing field. Even at low temperatures, where the temperature dependence of the FR in  $\text{CsNiF}_3$  clearly differs from that expected for a paramagnetic crystal, the amount of the rotation is only a few times larger than is usually observed in nonabsorbing paramagnets. In order to test the validity of expression (1) for a 1D ferromagnet-

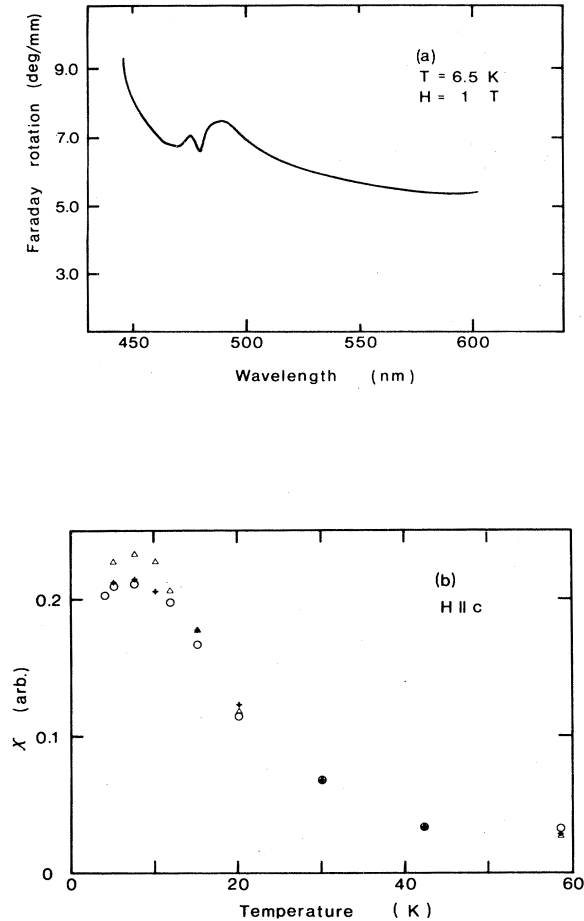


FIG. 10. (a) Dispersion of the Faraday rotation. Temperature dependences of the susceptibility from the Faraday rotation (pluses) and from the data of the Steiner (Ref. 25) (open circles) and of Dupas and Renard (Ref. 26) (open triangles).

ic material, the temperature dependence of  $\theta$  was measured from 4 to 60 K. The values of  $\chi$  obtained from these measurements were then normalized at 30 K to the susceptibility data of Steiner<sup>25</sup> and Dupas and Renard<sup>26</sup> for single-crystal specimens with  $\vec{H} \parallel \hat{c}$ . From a good agreement with these results, as shown in Fig. 10(b), we conclude that outside absorption regions the FR of a 1D ferromagnet is proportional to the magnetization. From a number of investigations, similar behavior is known to be valid in 2D and 3D ferromagnets.

#### IV. DISCUSSION

Using a classical approximation for the spin, Ebara and Tanabe<sup>13</sup> calculated the temperature dependence of the intensity of a hot-magnon band in a 1D ferromagnet. According to them the band intensity should increase in proportion to  $T$  at low temperatures and to saturate to a constant value at high temperatures.<sup>27</sup> It can be found from our experimental data that the intensity of the  $A$  band increases in proportion to  $T$  below 10 K and approaches a constant value above 15 K (Fig. 4). A qualitatively similar behavior is observed for the  $A'$  and  $G'$  bands, al-

though they are more difficult to investigate in details.

A one-magnon hot band is located on the low-energy side of an exciton band and is separated from it by the energy of the magnon. As can be seen from Figs. 3(a) and 8, the  $A$  and  $A'$  bands are situated on the low-energy sides of the  $B$  and the  $C$  bands. The separation between the  $A$  and  $C$  bands agrees very well with the energy ( $\sim 68 \text{ cm}^{-1}$ ) of the Brillouin-zone magnons when obtained from the magnon dispersion measured with the momentum transfer  $k_c$  along the 1D chains parallel to the hexagonal  $c$  axis.<sup>2</sup> Moreover, the  $A$ - $C$  band separation is almost the same as the  $A'$ - $B$  band separation. Therefore, if the  $B$  and  $C$  bands could be attributed to pure-exciton bands, it would be confirmed that the  $A'$  and  $A$  bands are one-magnon hot bands associated with the  $B$  and  $C$  exciton bands, respectively.

In contrast to the  $A$  and  $A'$  bands, the  $B$ - and  $C$ -band intensities decrease with increasing temperature, and the same temperature dependence is obtained for the  $G$  band, suggesting that the  $G$  band arises from the same origin as the  $B$  and  $C$  bands. Such a temperature dependence is expected for a cold-magnon band in antiferromagnets<sup>9</sup> and for an exciton band, as observed in BaMnF<sub>4</sub>.<sup>28</sup> The 3D antiferromagnetic ordering is present below  $T_N = 2.61 \text{ K}$  in CsNiF<sub>3</sub>, but the ordering seems to be too weak to induce the cold-magnon band since the interchain antiferromagnetic exchange energy  $J'$  is much smaller than the intrachain ferromagnetic exchange energy  $J$  ( $|J'/J| \sim 10^{-3}$ ).<sup>2</sup> The investigation of the pure-exciton band associated with the  ${}^3T_{2g}^a$  band in CsNiF<sub>3</sub> has shown that, when the temperature is increased, (1) the linewidth increases linearly, and (2) the peak position shifts linearly to lower energy.<sup>4</sup> It is also known that when a magnetic field applied parallel to the easy-magnetization plane is increased at 6 K, (1) the peak position shifts linearly to high energy, and (2) the half-width decreases by about  $2 \text{ cm}^{-1}$  in the variation from 0 to about 1.2 T but never changes above 1.2 T.<sup>5</sup> A quite similar behavior, including the field dependence measured at 7 K, was obtained in this work for the  $G$  band (see Figs. 5 and 6), indicating that the  $G$  band, and also the  $B$  and  $C$  bands, are attributable to exciton bands.

Cibert *et al.*<sup>4</sup> have related the line shift of the pure-exciton band of the  ${}^3A_{2g} \rightarrow {}^3T_{2g}^a$  spin-allowed transition to the magnetic energy of the ground state. Their value  $dE/dT = -0.44k_B$  agrees rather well with the shift of the peak position of the  $G$  band with temperature,  $-0.37k_B$ . The shift of the first moment of the  $G$  band was observed to be about 2 times this value, but it has a contribution from the  $G'$  band which partially overlaps the  $G$  band on its low-energy side. This interference does not exert much influence on the peak position of the band as it does on the band's first moment. The blue shift of the  $G$  line in an external magnetic field (Fig. 6) agrees well with the corresponding shift of the magnetic ground level induced by the field.

Several sharp peaks have been observed on the low-energy side of the  ${}^1T_{2g}^a$  band in other Ni<sup>2+</sup>-F<sup>-</sup> compounds, e.g., NiF<sub>2</sub>,<sup>20</sup> BaNiF<sub>4</sub>,<sup>18</sup> Rb<sub>2</sub>NiF<sub>4</sub>,<sup>16</sup> KNiF<sub>3</sub>,<sup>14,29</sup> and RbNiF<sub>3</sub>.<sup>30</sup> Of these compounds, the fine structure observed in BaNiF<sub>4</sub> and the KNiF<sub>3</sub> has been ascribed to

the phonon sidebands following a sharp zero-phonon line (pure-exciton line)<sup>18</sup> since the intervals between the prominent lines correspond to the phonon energy estimated from the infrared-adsorption measurements. On the other hand, the fine structure in the region of the bands *A* to *G* (shown in Fig. 3) does not exhibit a simple progression which could be related to phonon sidebands. Instead, in the MCD spectrum a progression due to phonon processes is found on the high-energy side of the *G* band. This suggests that the strong *G* band is attributable to the exciton line, as is the case of the strong band located on the lowest-energy side in BaNiF<sub>4</sub>.<sup>18</sup> In this way, the above assignment is confirmed for the *G* band.

The hot band *G'* is located at the energy of  $\sim 27 \text{ cm}^{-1}$  below the exciton band *G*. This separation is close to the magnon energy ( $\sim 22 \text{ cm}^{-1}$ ) obtained from inelastic-neutron-scattering measurements performed with  $k_a$  perpendicular to the chain in CsNiF<sub>3</sub>. In this case no dispersion was observed,<sup>2</sup> which is the opposite of the behavior of magnons with the wave vector  $k_c$  along the chain. The intensity of the *G'* band was found to decrease linearly when a magnetic field was increased from 0 to 4 T at 6.5 K. Similar behavior has been observed for the hot-magnon band in a 2D ferromagnet, Rb<sub>2</sub>CrCl<sub>4</sub>, where the magnons have an anisotropy gap at the Brillouin-zone center.<sup>12</sup> This suggests that the *G'* band is attributable to a hot-magnon band associated with magnons having a zone-center gap. For an easy-magnetization-plane 2D ferromagnet with negligible anisotropy (i.e., no zone-center gap in the magnon dispersion), the absorption intensity of a hot band varies approximately as  $T^2$  at low temperatures.<sup>31,32</sup> If, however, there is a zone-center gap, the intensity of the hot band begins to deviate from the  $T^2$  law as temperature becomes comparable to the gap energy.<sup>12</sup> A similar deviation is also expected for a 1D ferromagnet if there is a zone-center gap. In our easy-plane 1D ferromagnet CsNiF<sub>3</sub>, the intensity of the hot band *A* varies as  $T$  at low temperatures, in agreement with the theoretical calculation by Ebara and Tanabe,<sup>13</sup> and this law seems to hold even near 0 K (Fig. 4). This indicates that there is no zone-center gap in the magnon dispersion giving rise to the *A* band. This is consistent with the neutron scattering experiment<sup>2</sup> which shows the lack of the anisotropy gap in the magnon dispersion for  $k_c$  along the chains.

According to the theoretical calculation for the hot band in a 1D ferromagnet, the intensity gradually approaches a constant value as the temperature is increased. The *A*-band intensity, however, deviates rapidly from the  $T$  law above 11 K and takes a constant value above 15 K.

It is noted that the rapid change occurs near 12 K which is comparable to the intrachain ferromagnetic exchange energy  $J$  (see Fig. 4). One reason for such a discrepancy between the theoretical and experimental  $T$  dependences is probably that the presence of the 3D antiferromagnetic ordering below 2.61 K and the presence of short-range order up to about 50 K are neglected in the theoretical calculation.

## V. CONCLUSIONS

We note the following.

(1) At low temperatures a number of weak, sharp absorption bands are observed on the low-energy tail of the spin-forbidden transition  ${}^3A_{2g} \rightarrow {}^1T_{2g}^a$  in CsNiF<sub>3</sub>. Most of these lines gain their intensity from magnetic short-range interactions. Four lines are attributed to exciton lines by their intensity, which shows a linear decrease with the increasing temperature. The temperature dependence of the first and second moments of the *G* band, as well as their magnetic field dependences, are very similar to those of the pure-exciton band associated to the spin-allowed transition  ${}^3A_{2g} \rightarrow {}^3T_{2g}^a$ .<sup>4,5</sup> In the case of the exciton associated with the spin-forbidden transition to the  ${}^1T_{2g}^a$  state (*G* band), phonon contributions are also present, but these parameters still clearly reflect the magnetic properties of the ground state.

(2) A well-resolved hot-magnon band is observed above 3 K. The intensity of this band is found to increase linearly with increasing temperature until a saturation is reached at the temperature which corresponds to the intrachain ferromagnetic exchange energy  $J$ . This behavior agrees with the theoretical prediction of Ebara and Tanabe<sup>13</sup> and seems to be characteristic of a hot-magnon band in a 1D ferromagnet when the size of the anisotropy gap of the magnon energy is negligibly small.

(3) When measured with the external magnetic field along the *c* axis, the Faraday rotation of CsNiF<sub>3</sub> is shown to increase linearly with the field, at least up to 4.5 T. The temperature dependence of the susceptibility determined from the Faraday rotation agrees well with the results obtained by other methods.

## ACKNOWLEDGMENT

One of the authors (T.T.) thanks the Wihuri Physical Laboratory for support during his stay at the University of Turku.

\*Present address.

<sup>1</sup>D. Z. Babel, *Anorg. Allgem. Chem.* **396**, 117 (1969).

<sup>2</sup>M. Steiner, J. Villain, and C. G. Windsor, *Adv. Phys.* **25**, 87 (1976).

<sup>3</sup>A. Abragam and B. Bleaney, *Electron Paramagnetic Resonance of Transition Ions* (Clarendon, Oxford, 1970), p. 450.

<sup>4</sup>J. Cibert, Y. Merle d'Aubigné, J. Ferré, and M. Regis, *J. Phys. C* **13**, 2781 (1980).

<sup>5</sup>J. Cibert and Y. Merle d'Aubigné, *J. Magn. Magn. Mater.* **15-18**, 1059 (1980).

<sup>6</sup>J. Cibert and Y. Merle d'Aubigné, *Phys. Rev. Lett.* **46**, 1428 (1981).

<sup>7</sup>A. T. Abdalian, J. Cibert, and P. Moch, *J. Phys. C* **13**, 5587 (1980).

<sup>8</sup>D. Sell, R. L. Greene, and R. M. White, *Phys. Rev.* **158**, 489 (1976).

<sup>9</sup>K. Shinagawa and Y. Tanabe, *J. Phys. Soc. Jpn.* **30**, 1280 (1971).

<sup>10</sup>S. E. Schnatterly and M. Fontana, *J. Phys. (Paris)* **33**, 691 (1972).

- <sup>11</sup>D. J. Robbins and P. Day, *J. Phys. C* **9**, 867 (1976).
- <sup>12</sup>P. Day, E. Janke, T. E. Wood, and D. Woodwark, *J. Phys. C* **12**, L329 (1979).
- <sup>13</sup>K. Ebara and Y. Tanabe, *J. Phys. Soc. Jpn.* **36**, 93 (1974).
- <sup>14</sup>R. H. Petit, thesis, Université Pierre et Marie Curie, 1978.
- <sup>15</sup>J. Ferguson, *Aust. J. Chem.* **21**, 323 (1968).
- <sup>16</sup>J. Ferre, R. V. Pisarev, M. J. Harding, J. Badoz, and S. A. Kizhaev, *J. Phys. C* **6**, 1623 (1973).
- <sup>17</sup>I. Iio and K. Nagata, *J. Phys. Soc. Jpn.* **41**, 1550 (1976).
- <sup>18</sup>W. Kleeman, F. J. Schaefer, and J. Nouet, *J. Phys. C* **14**, 4447 (1981).
- <sup>19</sup>M. Kozielski, I. Pollini, and G. Spinolo, *Phys. Rev. Lett.* **27**, 1223 (1971).
- <sup>20</sup>P. Moch and M. Balkanski, in *Optical Properties of Ions in Crystals*, edited by H. M. Crosswhite and H. W. Moos (Interscience, New York, 1967), p. 313.
- <sup>21</sup>R. V. Pisarev, *Zh. Eksp. Teor. Fiz.* **49**, 1445 (1965) [*Sov. Phys.—JETP* **22**, 993 (1966)].
- <sup>22</sup>V. V. Druzhinin, R. V. Pisarev, and G. A. Karamysheva, *Fiz. Tverd. Tela (Leningrad)* **46**, 1445 (1965) [*Sov. Phys.—Solid State* **12**, 1789 (1971)].
- <sup>23</sup>J. Brynestad, H. L. Yakel, and G. P. Smith, *J. Chem. Phys.* **45**, 4632 (1966).
- <sup>24</sup>R. H. Petit, J. Ferre, and J. Nouet, *Physica* **86&88B**, 1213 (1977).
- <sup>25</sup>M. Steiner, *Z. Angew. Phys.* **32**, 116 (1971).
- <sup>26</sup>C. Dupas and J.-P. Renard, *J. Phys. C* **10**, 5057 (1977).
- <sup>27</sup>K. Ebara (private communication).
- <sup>28</sup>T. Tsuboi and W. Kleemann, *Phys. Rev. B* **27**, 3762 (1983).
- <sup>29</sup>R. V. Pisarev, J. Ferre, J. Duran, and J. Badoz, *Solid State Commun.* **11**, 913 (1972).
- <sup>30</sup>J. Tylicki, W. M. Yen, J. P. van der Ziel, and H. J. Guggenheim, *Phys. Rev.* **187**, 758 (1969).
- <sup>31</sup>A. K. Gregson, P. Day, A. Okiji, and R. J. Elliott, *J. Phys. C* **12**, 4497 (1976).
- <sup>32</sup>P. Day, *Colloq. Int. C.N.R.S.* **255**, 237 (1977).